

## **Contract Award - SPC # 004058**

*Title of Proposal: A Study of Sporadic E Layer Chemistry*

*Principal Investigator:* Professor John M. C. Plane  
School of Environmental Sciences  
University of East Anglia  
Norwich NR4 7TJ  
United Kingdom  
Telephone (44) 1603 593108  
Fax (44) 1603 507719  
Email: j.plane@uea.ac.uk

***EOARD Liaison Officer :* Lt. Col. David Burns**

### **Final Report**

The Contractor, University of East Anglia, hereby declares that, to the best of its knowledge and belief, the technical data delivered herewith under Contract No. 004058 is complete, accurate, and complies with all requirements of the contract.

Date 1 May 2002

Name and Title of Authorized Official: Prof. John Plane

*Start date:* 9 September 2000

*End date:* 30 April 2002

*Abstract:*

Sporadic *E* layers in the lower thermosphere play a very important role in radio communications. The lifetimes of these transient layers are largely controlled by the ion-molecule chemistry of metallic ions, particularly iron (Fe), that are produced by meteoric ablation. The aim of this project was to study the role of atomic oxygen in controlling the rate at which Fe<sup>+</sup> ions are neutralised. The rate coefficients for the reactions of Fe<sup>+</sup> with N<sub>2</sub>O, O<sub>2</sub> and N<sub>2</sub>, and the reactions of FeO<sup>+</sup> with CO and O, were measured using a fast flow tube coupled to a mass spectrometer, with Fe<sup>+</sup> ions produced by the pulsed laser ablation of an iron rod. Very good agreement was achieved with previous measurements of the first four reactions. The reaction of FeO<sup>+</sup> and O was found to be about 100 times slower than the Langevin limit. The results were then employed in a mesospheric model, which is now able to predict the top-side scale height of the atomic Fe layer and the ratio of Fe<sup>+</sup>/FeO<sup>+</sup> above 90 km in good accord with observations. Finally, a combination of emission spectroscopy and *ab initio* quantum theory was used to show that FeO<sup>+</sup> does not have an excited electronic state that would provide a suitable LIDAR probe in the atmospheric transmission window.

## Report Documentation Page

<b>Report Date</b> 21JUN2002	<b>Report Type</b> N/A	<b>Dates Covered (from... to)</b> 7SEP2000 - 07JAN2002
<b>Title and Subtitle</b> A Study of Sporadic E Layer Chemistry	<b>Contract Number</b>	
	<b>Grant Number</b>	
	<b>Program Element Number</b>	
<b>Author(s)</b> Plane, John	<b>Project Number</b>	
	<b>Task Number</b>	
	<b>Work Unit Number</b>	
<b>Performing Organization Name(s) and Address(es)</b> University of East Anglia Norwich NR4 7TJ United Kingdom	<b>Performing Organization Report Number</b>	
<b>Sponsoring/Monitoring Agency Name(s) and Address(es)</b> EOARD PSC 802 Box 14 FPO 09499-0014	<b>Sponsor/Monitor's Acronym(s)</b>	
	<b>Sponsor/Monitor's Report Number(s)</b>	
<b>Distribution/Availability Statement</b> Approved for public release, distribution unlimited		
<b>Supplementary Notes</b> The original document contains color images.		
<b>Abstract</b>		
<b>Subject Terms</b>		
<b>Report Classification</b> unclassified	<b>Classification of this page</b> unclassified	
<b>Classification of Abstract</b> unclassified	<b>Limitation of Abstract</b> UU	
<b>Number of Pages</b> 11		

## A. Introduction

Sporadic  $E$  layers are thin layers of concentrated plasma that occur in the lower thermosphere between about 90 and 120 km. They play a very important role in facilitating over-the-horizon radio transmission as well as obstructing space-to-ground communication, depending on the time-of-day and transmission frequency.<sup>1</sup> The objective of this proposal was to study the critical ion-molecule chemistry that determines the lifetimes of these transient events.

Measurements made with rocket-borne mass spectrometers have shown that sporadic  $E$  layers are largely composed of the metallic ions  $\text{Fe}^+$  and  $\text{Mg}^+$ , produced by meteoric ablation.<sup>2</sup> These ions (and an equal concentration of electrons) can be concentrated into layers only a few kilometres thick by various mechanisms, including wind shear, auroral precipitation, and gravity waves within the polar cap.<sup>3,4</sup> Above about 110 km, dielectric recombination (i.e.  $\text{Fe}^+ + \text{e}^- \rightarrow \text{Fe} + h\nu$ ) is the only significant route by which metallic ions can be removed. However, this is a very inefficient process with a rate coefficient of about  $10^{-11} \text{ cm}^3 \text{ s}^{-1}$ ,<sup>5</sup> corresponding to a lifetime for  $\text{Fe}^+$  of about 1 day even in a very intense sporadic  $E$  layer ( $fE_s = 10 \text{ MHz}$ ).

In contrast, ion-molecule reactions become important below 110 km, especially the reaction



We have recently measured the rate coefficient,  $k_1$ , and find that the reaction is very rapid below 100 km.<sup>6</sup> The resulting molecular ion can then undergo dissociative recombination with an electron:<sup>7</sup>



If this combination of reactions 1 – 2 were able to occur unchecked, then a sporadic  $E$  layer descending below 100 km would have a lifetime of only a few minutes, contrary to observation. In practice, atomic O must play a crucial role through the reaction



By competing with reaction 2 this limits the efficiency with which  $\text{Fe}^+$  is converted to Fe, and hence governs the lifetime of sporadic  $E$  in the 90 – 110 km region. In spite of its importance, the rate coefficient  $k_3$  has not been measured.

Plane *et al.*<sup>7</sup> have estimated  $k_3$  from detailed balancing with the reverse reaction, whose excitation function was measured in a molecular beam study.<sup>8</sup> This showed that  $k_3$  could be as low as  $2 \times 10^{-13} \text{ cm}^3 \text{ molecule}^{-1} \text{ s}^{-1}$  at lower thermospheric temperatures (200 K), whereas atmospheric modelling<sup>7</sup> of the neutral mesospheric Fe layer indicates a value of about  $7 \times 10^{-12} \text{ cm}^3 \text{ s}^{-1}$ . Simultaneous measurement of  $\text{Fe}^+$  and  $\text{FeO}^+$  in the lower thermosphere<sup>2</sup> also indicate a value for  $k_2$  around  $10^{-11} \text{ cm}^3 \text{ s}^{-1}$ . It is clear that  $k_3$  needs to be measured before the temporal behaviour of sporadic  $E$  can be properly modelled; this was the major focus of this project.

A secondary goal was to study the laser induced fluorescence (LIF) spectrum of  $\text{FeO}^+$  in the 520 – 550 nm region, where the molecule could have a strong  ${}^6\Sigma \leftarrow \text{X}{}^6\Sigma$  transition, by analogy with the isoelectronic molecule MnO. A recent photofragment study<sup>9</sup> has shown that  $\text{FeO}^+$  and MnO are strikingly similar molecules.

## B. Description of the Work

### Laboratory Measurements

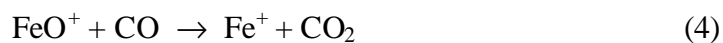
Figure 1 illustrates the apparatus employed for the project. A stainless steel fast flow tube was coupled to a two-stage quadrupole mass spectrometer configured for measuring positive ions. The source of  $\text{Fe}^+$  ions was the pulsed laser ablation of a rotating iron rod in the upstream section of the flow tube, using a frequency-doubled Nd:YAG laser (wavelength = 532 nm, energy  $\approx 20 \text{ mJ pulse}^{-1}$ ). This produced pulses of  $\text{Fe}^+$  (and also neutral Fe) that were entrained in a substantial flow of an inert gas (He), and swept down the tube at velocities in excess of  $10 \text{ m s}^{-1}$ . The pulses of ions were then detected by the mass spectrometer operating in pulse-counting mode, and interfaced to a multi-channel scalar. Figure 2 illustrates a sequence of  $\text{Fe}^+$  pulses recorded at different flow times, demonstrating the loss of  $\text{Fe}^+$  by diffusion to the walls of the tube. Because the pulse shapes are near Gaussian, the relative  $\text{Fe}^+$  concentration could be computed either from the pulse maximum or the integrated area of each pulse. The advantage of working with pulses is that the flow velocity of the ions down the tube can be measured precisely, whereas when using a continuous flow of ions, as in most conventional flow tubes, the plug velocity has to be corrected to account for the wall losses which create strong radial gradients.

The reactants ( $\text{N}_2\text{O}$ ,  $\text{O}_2$ , O etc.) were then admitted to the tube using either fixed inlets along the tube or a sliding injector. The latter was used to vary the distance (and hence time) during which the  $\text{Fe}^+$  and a reactant were in contact. Atomic O was generated by the microwave discharge of  $\text{N}_2$ , followed by titration with NO ( $\text{N} + \text{NO} \rightarrow \text{N}_2 + \text{O}$ ). The absolute concentration of O in the flow tube was measured by the classical titration with  $\text{NO}_2$ . The rate of loss of O on the flow tube walls was determined by adding NO just upstream of the optical port (see Figure 1), and observing chemiluminescence around 600 nm as the flow time was varied.

In order to search for possible electronic transitions of  $\text{FeO}^+$  in the visible (500 – 600 nm), ozone was added to the pulses of  $\text{Fe}^+/\text{Fe}$  just before the optical port. The resulting chemiluminescence was focused into a fibre optic and dispersed onto a CCD detector through a 0.5 m spectrometer with a choice of three gratings, providing resolution from 0.3 to 1.2 nm. Because strong chemiluminescence is generated from neutral Fe reacting with  $\text{O}_3$  (the “orange arc bands”), spectra were also recorded with  $\text{N}_2\text{O}$  added upstream. This reacts rapidly with  $\text{Fe}^+$  but not with Fe at room temperature,<sup>10</sup> providing a means of discriminating between emission due to  $\text{Fe}^+$  and Fe.

### Experimental Results

In order to characterise this novel system for studying ion-molecule reactions, the reactions of  $\text{Fe}^+$  with  $\text{N}_2\text{O}$ ,  $\text{O}_2$  and  $\text{N}_2$  were studied and compared with measurements made previously by the UEA group using a completely different technique.<sup>6,10</sup> As shown in Table 1, very satisfactory agreement was achieved. Before studying reaction 3, we also decided to study the reaction



This is analogous to the O atom reaction 3, but without the added complication of significant wall losses of the reactant down the tube.  $\text{FeO}^+$  was produced by the reaction



Figure 3 illustrates the results:  $\text{Fe}^+$  and  $\text{FeO}^+$  were monitored by the mass spectrometer, and their ratio is plotted against the ratio of  $[\text{N}_2\text{O}]$  to  $[\text{CO}]$ . This enabled  $k_4$  to be obtained directly relative to the rate coefficient for  $\text{Fe}^+ + \text{N}_2\text{O}$ , which is well known (Table 1 and ref. 10).

Reaction 3 was then studied by using reaction 5 to produce  $\text{FeO}^+$  and adding O through the sliding injector. The fraction of  $\text{Fe}^+$  relative to total  $\text{Fe}^+$  (that is, in the absence of either  $\text{N}_2\text{O}$  or O), was monitored as a function of both reactants. Figure 4 shows an experiment where the  $\text{N}_2\text{O}$  concentration was varied while the O atom concentration was fixed. This illustrates that there is a significantly higher fraction of  $\text{Fe}^+$  in the presence of atomic O, confirming that reaction 3 does indeed occur. In order to obtain  $k_3$ , a full kinetic model of the flow tube was developed, which included the wall losses of  $\text{Fe}^+$ ,  $\text{FeO}^+$  and O. Four data-sets under different conditions were then optimised to yield the value for  $k_3$  listed in Table 1. An example of the model fit is shown in Figure 4.

Figure 5 illustrates a chemiluminescence spectrum (blue line) produced by adding  $\text{O}_3$  to the  $\text{Fe}^+/\text{Fe}$  pulse. When  $\text{N}_2\text{O}$  was added to remove  $\text{Fe}^+$ , the resulting spectrum (red line) was found to be identical; this is confirmed by the absence of structure in the residual spectrum (dark green line, values multiplied by  $2 \times 10^4$ ). Indeed, for a series of spectra taken over the range 400 to 900 nm, the observed chemiluminescence was shown to arise exclusively from excited states of  $\text{FeO}$ .

### Theoretical Calculations

The experimental search for electronic transitions of  $\text{FeO}^+$  was complemented by a set of *ab initio* quantum calculations. The ground state of the ion was first optimised using the B3LYP hybrid density functional/Hartree Fock method with the 6-311+g(2d,p) basis set from within the Gaussian 98 suite of programs.<sup>12</sup> These reasonably high level calculations produced excellent agreement with measured parameters (shown in parenthesis, from ref. 9): bond length  $r_e = 1.641$  [1.648] Å, vibrational frequency  $\nu_e = 830$  [838±4]  $\text{cm}^{-1}$ , bond energy  $D_0(\text{Fe-O}^+) = 337$  [335±5]  $\text{kJ mol}^{-1}$ . Calculations were then performed on the first 10 excited states of  $\text{FeO}^+$ , using the configuration interaction (CI-Singles) method.<sup>12</sup> The vertical excitation energies and transition dipole moments are listed in Table 2.

In order to check the ability of the CI-Singles method to predict accurate excitation energies for these transition metal oxides, we performed analogous calculations at the same level of theory on  $\text{MnO}$  (isoelectronic with  $\text{FeO}^+$ ) and  $\text{FeO}$ , since the spectroscopies of both species are known. The results for these molecules are also listed in Table 2.

### Discussion

The rate coefficient for reaction 3 is about two orders of magnitude less than the typical Langevin limit for an ion-molecule reaction. This is in accord with the small reaction cross section for the reverse reaction,  $\text{Fe}^+ + \text{O}_2 \rightarrow \text{FeO}^+ + \text{O}$ , which

peaks at only  $1.7 \text{ \AA}^2$ .<sup>8</sup> Indeed, detailed balancing indicates that reaction 3 should proceed at only  $3 \times 10^{-13} \text{ cm}^3 \text{ molecule}^{-1} \text{ s}^{-1}$  at 296 K, a factor of 20 less than our experimental measurement (Table 1). This must indicate that reaction 3, which is exothermic by  $158 \pm 5 \text{ kJ mol}^{-1}$ , is able to access additional channels to yield products in excited states, including  $\text{Fe}^+(\text{}^4\text{F and } ^4\text{D})$  and/or  $\text{O}_2(\text{}^1\text{g})$ . Although we have so far only determined  $k_3$  at room temperature; the excitation function for the reverse reaction indicates that reaction 3 should have a very small temperature dependence.

Inspection of Table 2 shows that the CI-Singles method predicts excited states for MnO and FeO at 470 nm and 579 nm, respectively. These are in very good accord with the  ${}^6\Sigma \leftarrow X{}^6\Sigma$  transition of MnO at 520 nm, and the  ${}^5\Delta \leftarrow X{}^5\Delta$  transition of FeO around 580 nm (Figure 5). By contrast, the first excited state of  $\text{FeO}^+$  with a strongly allowed vertical transition is 4.7 eV above the ground state, corresponding to a transition in the UV. This result is supported by the absence in the spectrum in Figure 5 of chemiluminescence produced by reaction 1, which is sufficiently exothermic to populate electronic states of  $\text{FeO}^+$  up to 2.6 eV above the ground state. With no evidence for a suitable transition for  $\text{FeO}^+$  in the visible, it was decided not to attempt a laser induced fluorescence scan.

### Atmospheric Modeling

Figure 6 compares the annual average Fe layer at  $40^\circ\text{N}$  predicted by our 1-dimensional model<sup>7</sup> with a comprehensive set of lidar measurements from Prof. C. S. Gardner's group at U. of Illinois, Urbana-Champaign.<sup>13</sup> The scale height on the topside of the Fe layer is a sensitive test of the ion-molecule chemistry under consideration here. Excellent agreement was achieved by using the measured  $k_3$  from this study and fitting  $k_2$ , the rate coefficient for the dissociative recombination of  $\text{FeO}^+$  with an electron. The best fit value of  $k_2 = 5 \times 10^{-7} \text{ cm}^3 \text{ molecule}^{-1} \text{ s}^{-1}$  is in sensible accord with the measured rate coefficients for the analogous reactions of  $\text{NO}^+$  and  $\text{O}_2^+$ .

There is a limited set of simultaneous observations of  $\text{Fe}^+$  and  $\text{FeO}^+$  made by rocket-borne mass spectrometry in the lower thermosphere.<sup>2</sup> Prof. E. Kopp (U. of Bern) has made this rocket data available to us. Figure 7 illustrates profiles of the  $\text{Fe}^+/\text{FeO}^+$  ratio from four flights where  $\text{FeO}^+$  was above the detection limit. The ratio peaks at about 92 km, and is between 150 and 250, although with quite large uncertainty because the small concentrations of  $\text{FeO}^+$  are close to the detection limit. Our model currently predicts a ratio around 100 at 92 km. This is in sensible accord with the rocket data, since the ratio is very sensitive to the  $\text{O}_3/\text{O}$  ratio and these species have significant mixing ratio gradients in this region of the atmosphere.

Finally, the dramatic effect of this chemistry on the lifetime of  $\text{Fe}^+$  in a sporadic *E* layer is illustrated in Figure 8. This shows the lifetime of  $\text{Fe}^+$  against being neutralised to Fe, as a function of height and electron density. For critical frequencies ( $fE_s$ ) ranging from 1 to 10 MHz, the corresponding electron densities in a sporadic *E* layer vary from about  $1 \times 10^4$  to  $1 \times 10^6 \text{ cm}^{-3}$ . Figure 8 shows that very intense layers ( $fE_s > 8 \text{ MHz}$ ,  $[\text{e}^-] > 8 \times 10^5 \text{ cm}^{-3}$ ) will have lifetimes of about 1 hour at 100 km, and should be transient below this altitude. In contrast, weak layers ( $fE_s < 2 \text{ MHz}$ ,  $[\text{e}^-] > 5 \times 10^4 \text{ cm}^{-3}$ ), should have lifetimes of several hours down to 92 km.

### **Personnel**

The personnel involved in the project were Dr. Tomas Vondrak (senior research associate), Mr. Kenneth Woodcock (graduate student), and Prof. John Plane.

**Table 1.** Rate coefficients (296 K) determined during this project.

Reaction	Rate coefficient <sup>a</sup>	
	This study	Previous work
$\text{Fe}^+ + \text{N}_2\text{O} \rightarrow \text{FeO}^+$	$(4.99 \pm 0.24) \times 10^{-11}$	$(4.47 \pm 0.94) \times 10^{-11}$ <sup>b</sup>
$\text{Fe}^+ + \text{N}_2 + \text{He} \rightarrow \text{FeN}_2^+ + \text{He}$	$(2.37 \pm 0.20) \times 10^{-30}$	$(2.10 \pm 0.32) \times 10^{-30}$ <sup>c</sup>
$\text{Fe}^+ + \text{O}_2 + \text{He} \rightarrow \text{FeO}_2^+ + \text{He}$	$(3.54 \pm 0.24) \times 10^{-30}$	$(4.17 \pm 0.23) \times 10^{-30}$ <sup>c</sup>
$\text{FeO}^+ + \text{CO} \rightarrow \text{Fe}^+ + \text{CO}_2$	$(1.49 \pm 0.06) \times 10^{-10}$	$(2.05 \pm 0.2) \times 10^{-10}$ <sup>d</sup>
$\text{FeO}^+ + \text{O} \rightarrow \text{Fe}^+ + \text{O}_2$	$(6 \pm 2) \times 10^{-12}$	Not measured

<sup>a</sup> Units: bimolecular reactions,  $\text{cm}^3 \text{ molecule}^{-1} \text{ s}^{-1}$ ; termolecular,  $\text{cm}^6 \text{ molecule}^{-2} \text{ s}^{-1}$

<sup>b</sup> Ref. 10. <sup>c</sup> Ref. 6. <sup>d</sup> Ref. 11

**Table 2.** Excited states of  $\text{FeO}^+$ , MnO and FeO, calculated using the CI-Singles method with the 6-311+g(2d,p) basis set. The vertical excitation energy, corresponding wavelength and transition dipole moment (f) are shown. The highlighted transitions indicate the first excited state of each molecule with a strongly-allowed transition from the ground state.

	$\text{FeO}^+$ excited states	MnO excited states	FeO excited states
1	0.21 eV 6048 nm f=0.0000	0.21 eV 5794 nm f=0.0000	0.052 eV 23979 nm f=0.0000
2	0.30 eV 4185 nm f=0.0000	0.92 eV 1346 nm f=0.0015	0.052 eV 23979 nm f=0.0000
3	0.38 eV 3289 nm f=0.0000	2.64 eV 470 nm f=0.2234	0.30 eV 4185 nm f=0.0000
4	0.88 eV 1414 nm f=0.0001	2.75 eV 450 nm f=0.2257	1.00 eV 1238 nm f=0.0000
5	1.09 eV 1136 nm f=0.0000	3.39 eV 365 nm f=0.1786	1.00 eV 1238 nm f=0.0000
6	1.48 eV 837 nm f=0.0000	4.04 eV 306 nm f=0.0010	1.24 eV 1004 nm f=0.0000
7	4.70 eV 263 nm f=0.0056	4.47 eV 277 nm f=0.0000	1.61 eV 769 nm f=0.0001
8	5.20 eV 238 nm f=0.0041	4.47 eV 277 nm f=0.0000	1.61 eV 769 nm f=0.0001
9	5.33 eV 232 nm f=0.0012	4.78 eV 260 nm f=0.0233	1.88 eV 661 nm f=0.0000
10	5.37 eV 231 nm f=0.0144	5.59 eV 222 nm f=0.0295	2.14 eV 579 nm f=0.0559

## References

1. Smith, E. K., and S. Matsushita, *Ionospheric Sporadic E*, Pergamon, Tarrytown, NY, 1962.
2. Kopp, E., P. Eberhardt and U. Herrmann, Positive ion composition of the high-latitude summer *D* region with noctilucent clouds, *J. Geophys. Res.*, **90**, 13041-13053, 1995.
3. Chimonas, G., and W. I. Axford, "Vertical movement of temperate-zone sporadic E layers", *J. Geophys. Res.*, **73**, 111-117, 1968.
4. MacDougall, J. W., J. M. C. Plane, and P. T. Jayachandran, Polar cap Sporadic-E: Part 2, Modeling, *J. Atmos. Sol. Terr. Phys.*, in press.
5. Nahar, S. N., M. A. Bautista and A. K. Pradhan, Electron-ion recombination of neutral iron, *Astrophys. J.*, **479**, 497 – 503, 1997.
6. Rollason, R. J. and J. M. C. Plane, A Kinetic Study of the Reactions between Fe<sup>+</sup> ions and O<sub>3</sub>, O<sub>2</sub> and N<sub>2</sub>, *J. Chem. Soc., Far. Trans.*, **94**, 3067-3075, 1998.
7. Plane, J. M. C., R. M. Cox and R. J. Rollason, Metallic Layers in the Mesopause and Lower Thermosphere Region, *Adv. Space Res.*, **24**, 1559-1570, 1999.
8. Loh, S. K., E. R. Fisher, L. Lian, R. H. Schultz, and P. B. Armentrout, State-specific reactions of Fe<sup>+</sup>(<sup>6</sup>D, <sup>4</sup>F) with O<sub>2</sub> and c-C<sub>2</sub>H<sub>4</sub>O: *D*<sup>0</sup><sub>0</sub>(Fe<sup>+</sup>-O) and effects of collisional relaxation, *J. Phys. Chem.*, **93**, 3159-3167, 1989.
9. Husband, J., F. Aguirre, P. Ferguson and R. B. Metz, Vibrationally resolved photofragment spectroscopy of FeO<sup>+</sup>, *J. Chem. Phys.*, **111**, 1433-1437, 1999.
10. Plane J. M. C., and R. J. Rollason, A Kinetic Study of the Reactions between Fe(<sup>5</sup>D) and Fe<sup>+</sup>(<sup>6</sup>D) with N<sub>2</sub>O over the temperature range 294 – 850 K, *J. Chem. Soc., Far. Trans.*, **92**, 4371-4376, 1996.
11. Baranov V., G. Javahery, A. C. Hopkinson, D. K. Bohme, Intrinsic coordination properties of iron in FeO<sup>+</sup>: Kinetics at 294±3 K for gas-phase reactions of the ground states of Fe<sup>+</sup> and FeO<sup>+</sup> with inorganic ligands containing hydrogen, nitrogen, and oxygen, *J. Am. Chem. Soc.* **117**, 12801-12809, 1995.
12. Frisch, M. J., G. W. Trucks, H. B. Schlegel, G. E. Scuseria, M. A. Robb *et al.*, Gaussian 98, Revision A. 7, Gaussian, Inc., Pittsburgh PA, 1998.
13. Helmer, M., J.M.C. Plane, J. Qian and C.S. Gardner, A model of meteoric iron in the upper atmosphere, *J. Geophys. Res.*, **103**, 10913-10925, 1998.

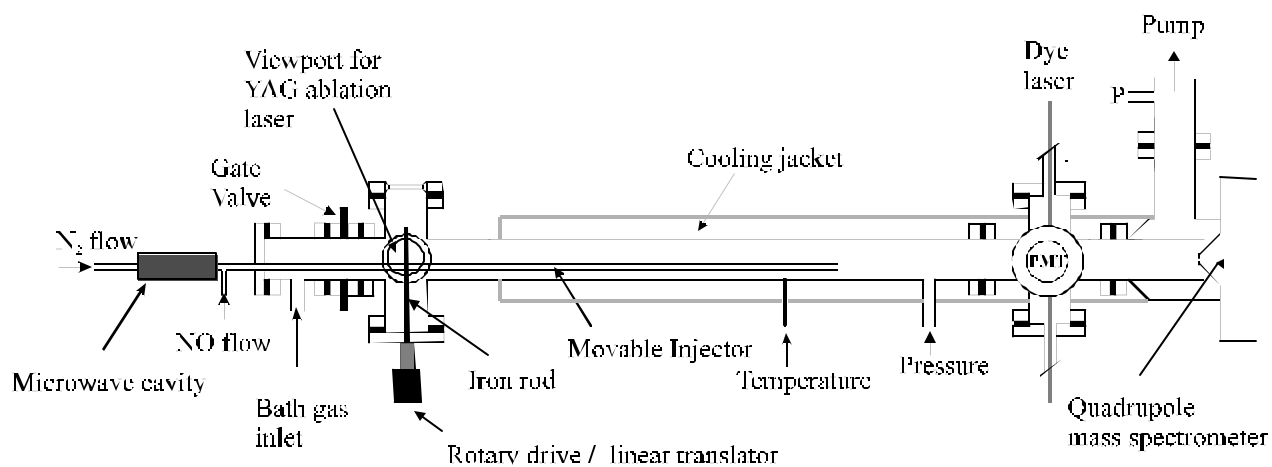


**Figure 1.** Schematic diagram of the fast flow tube/pulsed laser ablation system for studying the kinetics of ion-molecule reactions of Fe-containing species.

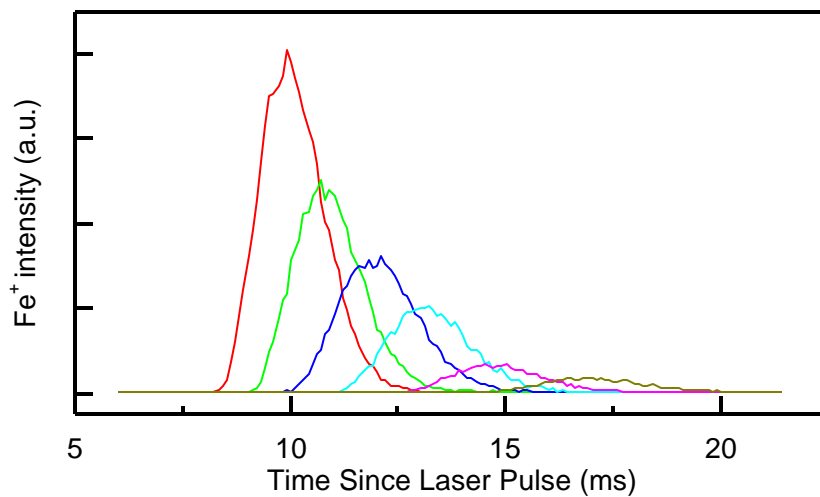


**Figure 2.** Time profiles of  $\text{Fe}^+$  pulses for different bath gas (He) flows. From left to right: 5500 sccm, 5000 sccm, 4500 sccm, 4000 sccm, 3500 sccm and 3000 sccm. The total drift length is 89.5 cm.

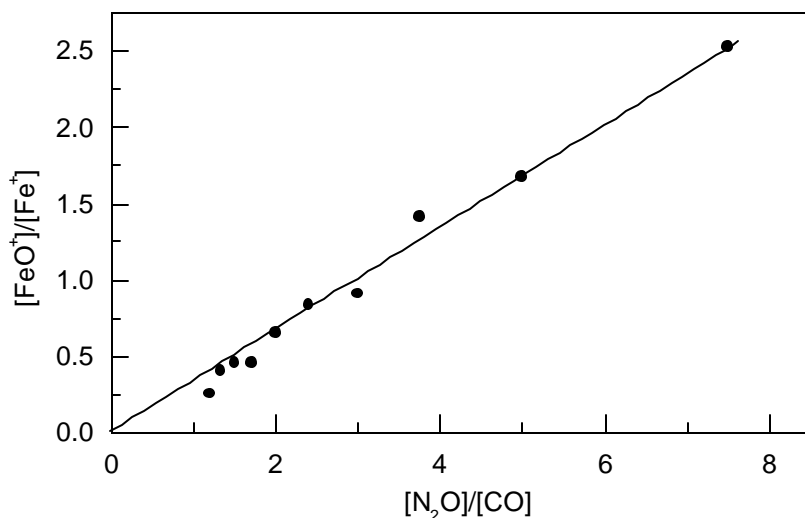


**Figure 3.** Study of the reaction between  $\text{FeO}^+$  and CO. The  $\text{FeO}^+/\text{Fe}^+$  ratio detected at the downstream end of the flow tube is plotted against the ratio of  $\text{N}_2\text{O}$  and CO. The slope yields the rate coefficient relative to that for  $\text{Fe}^+ + \text{N}_2\text{O}$ .  $\text{N}_2\text{O}$  and CO were added 8.5 cm and 13.5 cm downstream of the  $\text{Fe}^+$  source, respectively. The total drift distance was 89.5 cm. The flow tube pressure was 1.2 Torr and the total gas flow was 3500 sccm.

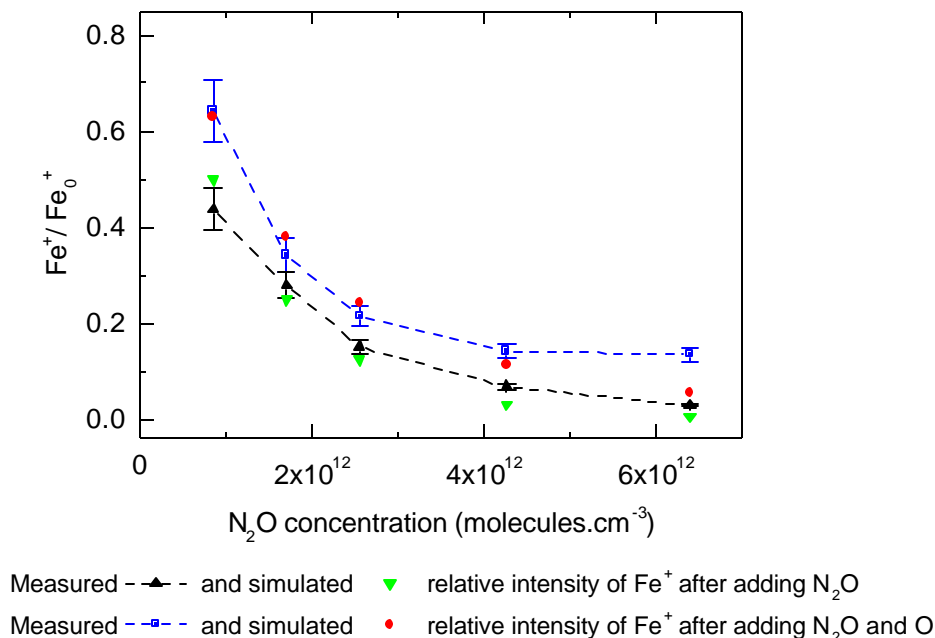


**Figure 4.** Study of the reaction between  $\text{FeO}^+$  and atomic O. The ratio of  $\text{Fe}^+$  in the presence of  $\text{N}_2\text{O}$ , versus the total  $\text{Fe}^+$  in the absence of reactants, is plotted against the  $\text{N}_2\text{O}$  concentration (black points). The experiment is then repeated with  $3.7 \times 10^{13} \text{ cm}^{-3}$  of atomic O added (blue points). The model simulations are the green and red points, respectively.

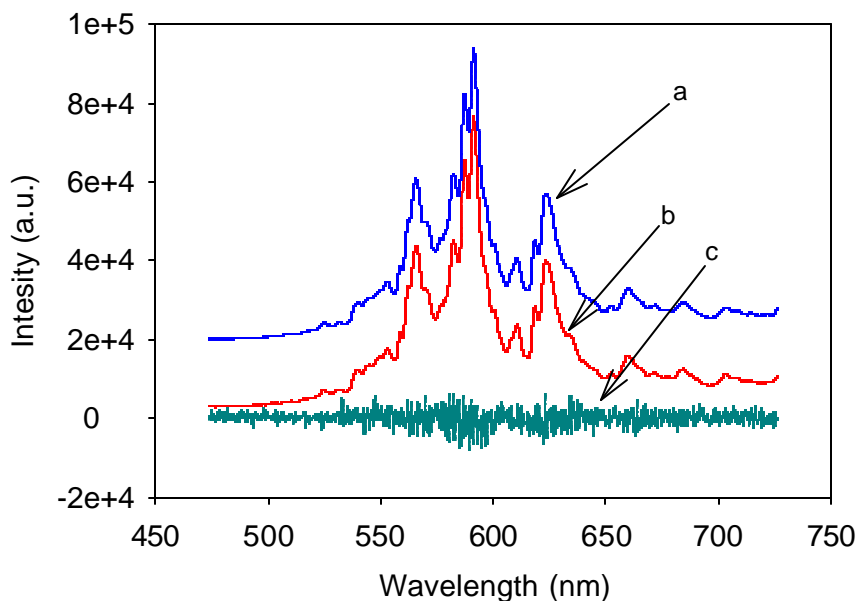


**Figure 5.** Emission spectra recorded when  $\text{O}_3$  ( $3 \times 10^{13} \text{ cm}^{-3}$ ) is added to the pulse of  $\text{Fe}^+/\text{Fe}$  just before the optical detection port at the downstream end of the flow tube. The spectra were recorded with 1.2 nm resolution on a CCD detector: (a) chemiluminescence from  $\text{Fe}$  and  $\text{Fe}^+ + \text{O}_3$ ; (b) chemiluminescence from  $\text{Fe} + \text{O}_3$ , with the  $\text{Fe}^+$  removed by addition of  $\text{N}_2\text{O}$  upstream; (c) the residual (a) – (b), multiplied by  $2 \times 10^4$ , demonstrating no identifiable chemiluminescence due to  $\text{Fe}^+ + \text{O}_3$  producing excited states of  $\text{FeO}^+$ .

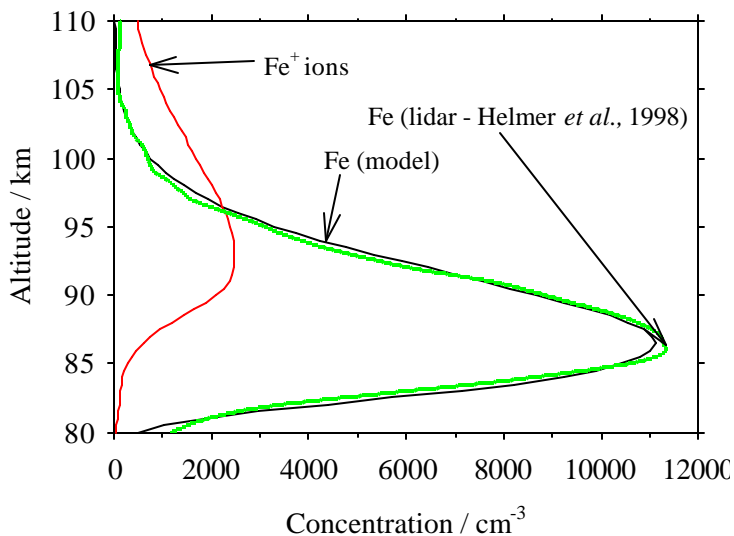


**Figure 6.** The annual average layer of atomic  $\text{Fe}$  at  $40^\circ\text{N}$ , comparing lidar observations from the University of Illinois (green line) with the UEA 1-D model prediction (black line). The predicted profile of  $\text{Fe}^+$  (red line) is also shown.

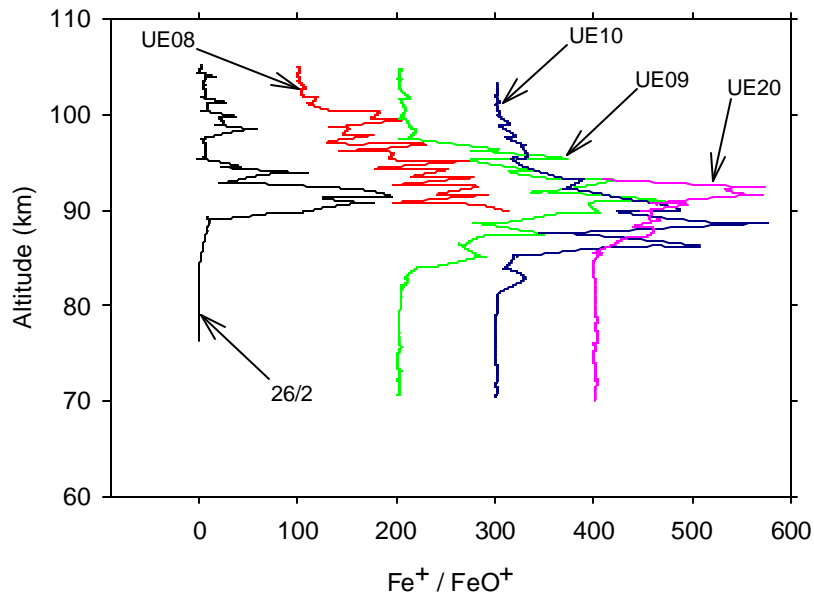


**Figure 7.** The ratio of  $\text{Fe}^+/\text{FeO}^+$  measured by rocket-borne mass spectrometry (Prof. E. Kopp, U. of Bern). For the sake of clarity, each flight is shifted by 100 units. The rocket flights were made during twilight at high latitudes during summer.

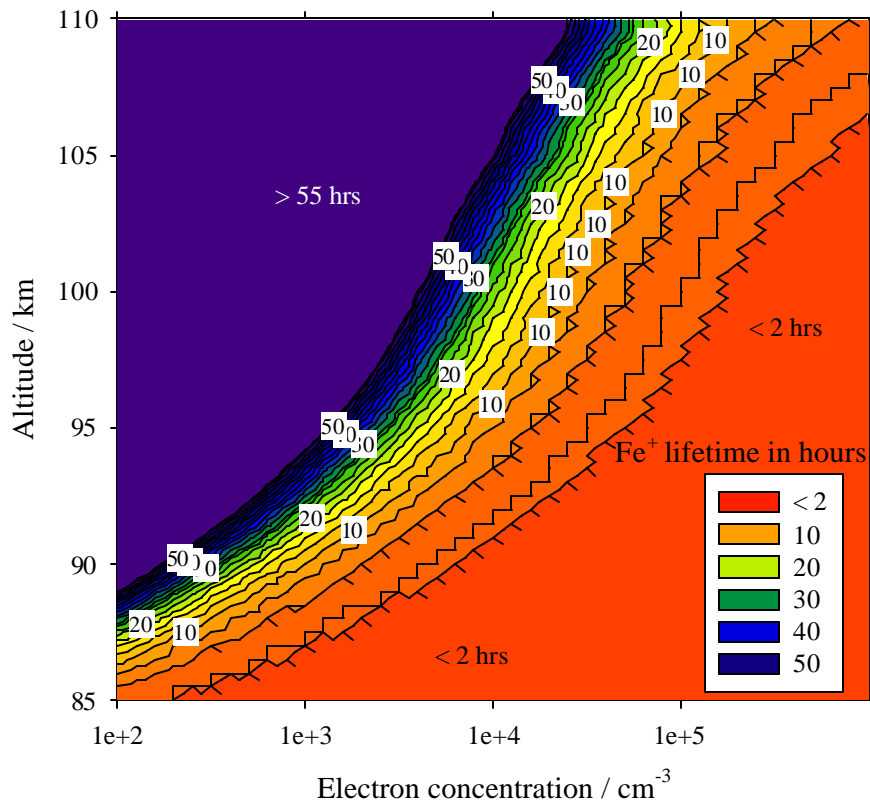


**Figure 8.** The predicted lifetime of  $\text{Fe}^+$ , with respect to being neutralised to Fe, as a function of height and electron concentration. Conditions: January, midnight,  $40^\circ\text{N}$ .